Dispersed-Phase Holdup in a Rotating Disk Extraction Column

E. Y. KUNG and R. B. BECKMANN
Carnegie Institute of Technology, Pittsburgh, Pennsylvania

A study has been made of the effect of column geometry and flow condition upon the dispersed-phase holdup in an rotating disk type of extraction column. Variables investigated were stator opening, disk diameter, compartment height, rotor speed, and flow rates of the dispersed and continuous phases. The toluene-water system, with the toluene dispersed, was used throughout the study. The radio-isotope technique was used to measure the dispersed-phase holdup.

Results of this study as well as those of earlier investigators have been used to expand upon the design equations proposed by Logsdail, Thornton, and Pratt for estimating flooding rates and dispersed-phase holdup in rotating disk columns. Modifications to increase the accuracy of prediction of these equations have also been suggested, while possible limitations in their application have been indicated.

The rotating disk column was patented by G. H. Reman (*1*), who claimed that the column has a high volumetric efficiency, is of straightforward construction, is cheaper to build for equivalent capacities than other existing apparatus of comparable efficiency, and can be scaled up to comparatively large diameters without undue loss in efficiency. The column consists of a number of compartments formed by a series of stator rings, with a rotating disk centered in each compartment and supported by a rotating shaft. The lighter liquid enters the column at the bottom and flows upward countercurrently to the descending heavier liquid. One of the liquids is dispersed by the rotating disks and flows through the column in a toroidal pattern.

Reman and Olney (*2*), Reman and van de Vusse (*3, 4*), and Vermijs and Kramers (*5*) have published considerable operational and mass transfer data on specific small and large rotating disk extraction columns. Logsdail, Thornton, and Pratt (*6*) studied flooding rates for a 3-in. diameter rotating disk column in terms of column variables and physical properties. In a few cases the dispersed-phase holdup below and/or at the flood point was determined. Mass transfer data were also obtained. The column variables studied included stator opening at 2.0 and 2.25 in. disk diameter at 1.0, 1.5, and 2.0 in., compartment height at 0.50, 1.0, 2.0, and 4.0 in. and rotor speed over the range of 500 to 1,600 rev./min. Water was used throughout as the continuous phase, while toluene, butyl acetate, iso-octane, white spirit, and benzene were used as the dispersed phases.

The authors observed during operations of their rotating disk column that the size of the dispersed-phase droplet was independent of the phase flow rates and the dispersed-phase holdup. Using semitheoretical considerations they postulated that for such cases the phase flow rates and holdup for a specific system at a given column geometry and rotor speed can be related by the equation

$$\frac{V_d}{X} + \frac{V_c}{(1-X)} = \overline{V}_N(1-X) \quad (1)$$

where $\overline{V}_N$ is regarded as the mean vertical component of velocity of the droplets with respect to the continuous phase.

The authors further asserted that at flooding point the flow rates reached a maximum, and introduced this condition into Equation (1) by differentiating and setting (dV_d/dX) and (dV_c/dX) equal to zero. This results in the following equations:

$$V_{d(f)} = 2\overline{V}_N X_f^2 (1 - X_f) \quad (2)$$

$$V_{c(f)} = \overline{V}_N (1 - X_f)^2 (1 - 2X_f) \quad (3)$$

which relate the phase flow rates at flooding to the corresponding holdup, X_f. A relation between X_f and the flow ratio $V_{d(f)}/V_{c(f)}$ was then obtained by eliminating $\overline{V}_N$ between Equations (2) and (3); thus

$$X_f = \frac{(L^2 + 8L)^{0.5} - 3L}{4(1-L)}$$

where

$$L = \frac{V_{d(f)}}{V_{c(f)}} \quad (4)$$

Logsdail, Thornton, and Pratt evaluated values of $\overline{V}_N$ from their data of flooding rates by means of Equations (2) and (4). In those cases, where the dispersed-phase holdup was also determined at the flood point, $\overline{V}_N$ was also estimated graphically from Equation (1) and was shown to be in good agreement with the values evaluated by the first method. The few holdup measurements made below the flood point also gave values of $\overline{V}_N$ in agreement with those obtained by the other methods.

A relationship between the values of $\overline{V}_N$ thus evaluated and the physical properties of the system, the column geometry, and the rotor speed was then developed through dimensional analysis. The final expression was

$$\left(\frac{\overline{V}_N \mu_c}{\gamma}\right) = 0.012 \left(\frac{\Delta\rho}{\rho_c}\right)^{0.90}$$

E. Y. Kung is with Jones and Laughlin Steel Corporation, Pittsburgh, Pennsylvania.

$$\left(\frac{g}{dpN^2}\right)^{1.0}\left(\frac{di}{dp}\right)^{2.3}\left(\frac{h}{dp}\right)^{0.90}\left(\frac{dp}{dc}\right)^{2.7} \quad (5)$$

The primary objective of this investigation is to determine the effect of column geometry and operating flow rates upon the applicability of Equations (1) through (5) and to determine, if possible, the limits of their applicability for designing or for estimating the performance of rotating disk columns.

DESCRIPTION OF EQUIPMENT

The specific column geometries studied are summarized in Table 1. The column was constructed as shown in Figure 1 from a 4-ft. section of 6 in. I.D. pyrex glass pipe, bolted at the two ends to ½ in. thick plates through flanged end pieces. The shaft was driven by a ½-hp. motor, and variations in speed were obtained through a system of pulleys. The stator rings and rotor disks were both made of stainless steel. Eight stators with the same opening were used in constructing the column, forming seven compartments. The stators were supported by four ¼ in. stainless steel stator rods, and polyethylene tubing was placed between the stator rings and glass column to prevent bypassing of the liquids due to the irregular contour of the glass pipe.

The equipment used for measuring the dispersed-phase holdup by the radioisotope technique was similar to that used by Markas (7) in studying the performance of spray and packed liquid-liquid extraction columns. Gamma radiation emitted from tagged toluene droplets were measured by means of a scintillation counter. The scintillation counting circuit consisted of a radiation counting rate meter, a scintillation counter, a six-stage binary scaler, an electric timer, a mechanical register, and a constant voltage transformer. The scintillation counter was positioned to view the equivalent of the central compartment. A rotating traverse was made to assure proper averaging and also to assure that a time-stable equilibrium was reached.

Industrial-pure toluene and distilled water were used, while the radioisotope used was Iodine-131 in the form of Raolein, which is iodinated triolein diluted with a special ampule grade of peanut oil. Periodic system replacements were made of both toluene and distilled water.

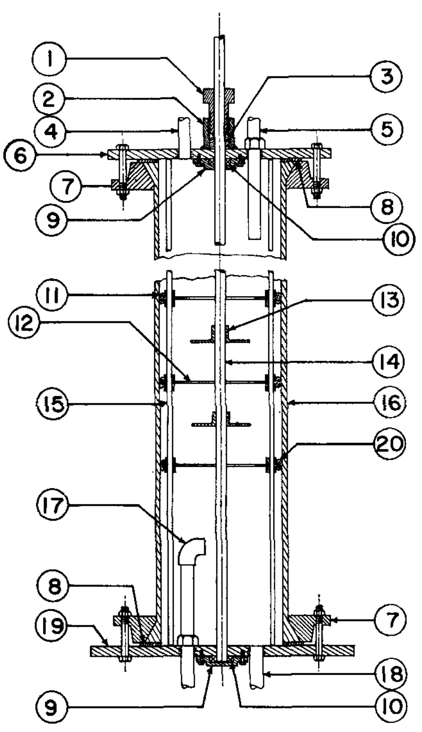

Fig. 1. Construction details of rotating disk extraction column.

1 = packing nut, 2 = stuffing box, 3 = packing, 4 = toluene outlet, 5 = water inlet, 6 = top plate, 7 = flanges, 8 = Teflon gasket, 9 = bearing housings, 10 = ball bearings, 11 = set screw collars, 12 = stator rings, 13 = rotor disks, 14 = rotating shaft, 15 = stator rods, 16 = column, 17 = toluene inlet, 18 = water outlet, 19 = bottom support plate, 20 = polyethylene tubing.

EXPERIMENTAL PROCEDURE

Determination of Holdup

The holdup of the dispersed phase was determined at 0 and 460 rev./min. for all column geometries listed in Table 1 except units B, H, and I. For units B and H the dispersed-phase holdup was determined at the following rotor speeds: 0, 200, 460, and 600 rev./min. Unit I was used only in flooding velocity determination. All runs at 0 rev./min. except those for units B and H were made at zero continuous-phase flow. All other runs were made with varying dispersed-phase velocity at zero continuous-phase velocity and with varying continuous-phase velocities at constant dispersed-phase velocities of 20.44 and 40.87 ft./hr.

Before the operation was started, the liquids were saturated with one another. The Raolein containing the I-131 (about 9 mcuries.) was placed in the toluene feed drum, and the liquids were then circulated through the column for a period of at least 6 hr. to insure that all of the isotope was uniformly distributed throughout the solvent phase.

Each determination was carried out by filling the column with the continuous aqueous phase and setting the rotor speed to the desired value. The phase flow rates were then adjusted. The two-phase interface was maintained at 3 in. below the top end plate. Operation was then held constant and the scintillation counting circuit turned on. The radiation rate was observed from the binary scaler and the mechanical register, the flow rates were observed from the rotameters, and the rotor speed was measured by a portable tachometer in contact with the rotating shaft.

To calibrate these radiation rates in terms of holdup, that is the fractional part of the total volume within the column or the compartments that is occupied by the dispersed-phase droplets, the column was filled only with a stationary column of tagged toluene. The radiation emitted under these conditions was recorded. The ratio of the two radiation intensities (with suitable corrections) yielded directly the fractional holdup within the column or compartments under operating conditions.

Determination of Flooding Rates

Flooding rates were determined at various rotor speeds for columns B, I, and J (Table 1). Each determination was carried out according to the experimental procedure used by Markas (7), the only additional operating parameter being rotor speed.

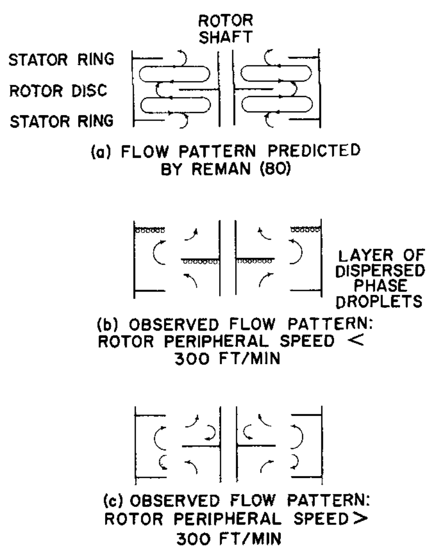

Fig. 2. Dispersed phase flow patterns in a rotating disk extraction column.

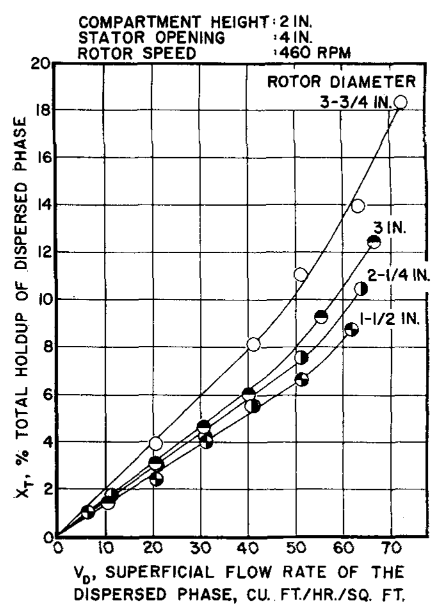

Fig. 3. Effect of rotor diameter on dispersed-phase holdup.

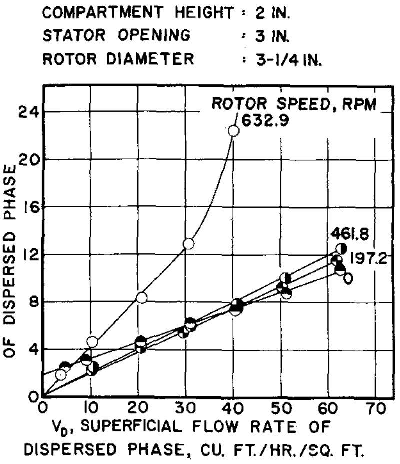

Fig. 4. Effect of rotor speed on dispersed-phase holdup.

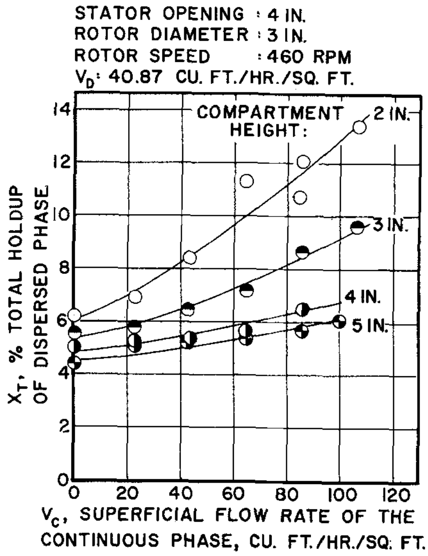

Fig. 5. Effect of compartment height on dispersed-phase holdup.

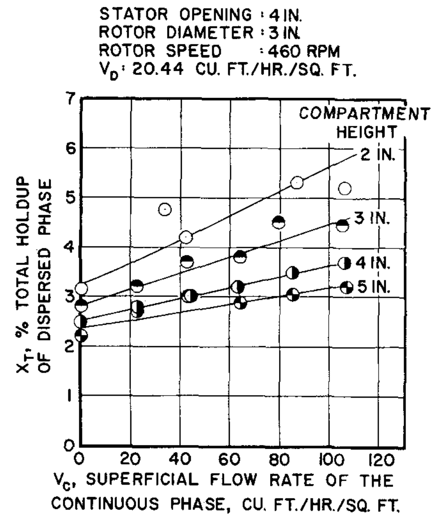

Fig. 6. Effect of compartment height on dispersed-phase holdup.

DISCUSSION OF RESULTS

Column Behavior

Figure 2*a* presents a schematic sketch of the flow pattern of dispersed-phase droplets rising through a compartment of a rotating disk column as outlined by Reman (*1*). As suggested in the figure the flow of liquid in a rotating disk column consists of three movements of the liquid. Basically there is a countercurrent flow of the two phases caused by a density difference. Apart from this countercurrent flow the flow of liquid consists of a rotation of the whole liquid mass on which there is superimposed a slower movement of the liquid from the shaft towards the wall of the column in the vicinity of the rotor disks, and from the wall back towards the shaft in the vicinity of the stator rings. Thus the flow of the liquid, aside from the countercurrent flow of the phases, is toroidal. This toroidal flow causes local recirculation, or back mixing, of both liquids within each compartment, and only portions of the liquid taking part in this flow pass on to the next compartment by gravity. The flow of the liquid resulting from the rotation of the rotor disks causes one of the liquids to become reduced to a very fine state and dispersed because of the shearing stresses accompanying this flow. For a given column geometry the size of the droplets formed is controlled in each compartment by rotor speed.

The actual flow pattern of dispersed-phase droplets may differ somewhat from that suggested by Figure 2*a*. It was observed during the experimental runs in this investigation that the flow of the droplets followed two general patterns. Schematic sketches of these two general flow patterns of the droplets are shown in Figures 2*b* and *c*, respectively. In general at rotor peripheral speeds less than 300 ft./min., except at the vicinity of the flood point, the flow of the liquid is countercurrent with a rotation of the whole liquid mass around the rotor shaft. The movement of the liquid from the shaft toward the wall of the column in the vicinity of the rotor disks, and from the wall back toward the shaft in the vicinity of the stator rings, is not evident under these conditions, and there appears to be very little back mixing. This explains the absence in Figure 2*b* of the recirculation loops, which appeared in Figure 2*a*.

Also as indicated in Figure 2*b*, for all runs at rotor peripheral speeds less than 300 ft./min. layers of dispersed-phase droplets were generally observed to be trapped under the stator rings and/or rotor disks. The amount of droplet entrapment however was a function of the column geometry, rotor speed and the liquid flow rates.

At rotor peripheral speeds higher than 300 ft./min., and/or at the vicinity of the flood point for all runs, all three movements of the liquid, as described in Reman (*1*), can be observed, and back mixing became generally prominent, with the severity of the back mixing being a function of the column geometry, rotor speed, and phase flow rates. Figure 2*c* is similar to Figure 2*a* except that the former underscored the difference in quantity between portion of the liquid which recirculated and the main body of the flow of the liquid. However at the vicinity of the flood point the flow pattern of the dispersed phase approached that represented by Figure 2*a*.

TABLE 1. COLUMN DIMENSIONS

Unit	Compartment height, (in.)	Stator opening, (in.)	Disk diameter, (in.)
A	2.0	4.0	3.75
B	2.0	4.0	3.0
C	2.0	4.0	2.25
D	2.0	4.0	1.50
E	2.0	3.25	1.50
F	2.0	2.50	1.50
G	2.0	1.75	1.50
H	2.0	3.25	3.0
I	3.0	4.0	3.75
J	3.0	4.0	3.0
K	4.0	4.0	3.0
L	5.0	4.0	3.0

Note—The same column section, with an inside diameter of 6 in. and column length of 48 in., was used throughout.

Dispersed-Phase Holdup

The range of data taken in this investigation covered stator openings at 1-¾, 2-½, 3-¼, and 4 in.; disk diameters at 1-½, 2-¼, 3, and 3-¾ in.; and compartment heights of 2, 3, 4, and 5 in.* A 6-in. I.D. column was used throughout, while rotor speed was varied from 0 to 632.9 rev./min. Figure 3 shows the effect of disk diameter on the dispersed-phase holdup at a zero continuous phase flow rate. Holdup expressed as the volume percent of the column volume occupied by the dispersed phase is plotted vs. the dispersed phase flow rate. As indicated in Figure 3 the holdup increased with decreasing stator opening and compartment height and increasing disk diameter and rotor speed. Figure 3 also shows that the holdup increased linearly with flow rate of the dispersed phase until the loading point was reached. Above the loading point the holdup increased more sharply with increasing dispersed phase flow rate. The effect of compartment height and stator opening on dispersed-phase

* Data can be obtained on inter-library loan from Carnegie Institute of Technology.

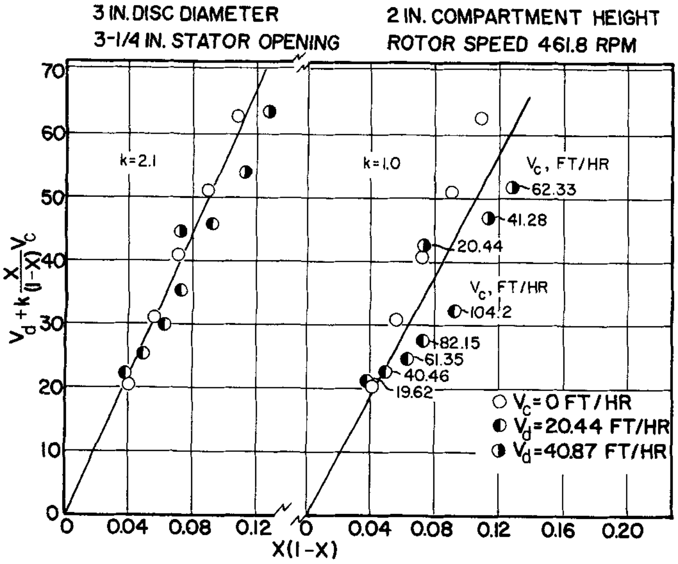

Fig. 7. Correlation of characteristic velocity.

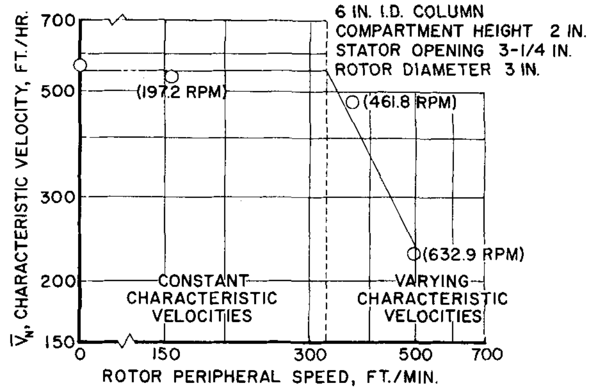

Fig. 8. Characteristic velocity variation with rotor peripheral speed.

holdup follows a similar behavioral pattern. The effect of rotor speed on dispersed-phase holdup at a zero continuous phase flow rate is shown in Figure 4. It is interesting to note that in Figure 4 the straight line representing the holdup data below the loading point for the runs at 0 rev./min. with 2-in. compartment height, 3-¼-in. stator opening, 3-in. disk diameter, and zero continuous-phase flow does not extrapolate to the origin, as do the lines representing holdup data for the runs at other than 0 rev./min. with the same operating conditions. The same phenomenon was observed for runs at other column geometries where the disk diameters are large or the stator openings small. A probable explanation lies in the observation that, during the runs at 0 rev./min., zero continuous-phase flow, and very low dispersed phase flow rates for such column geometries, dispersed-phase droplets were trapped permanently under either the rotor disks or the stator rings, while during runs under the same conditions at other than 0 rev./min. the dispersed phase trapped under the disks or stators was either mobile or negligible in quantity.

Holdup vs. continuous phase flow rate, at constant dispersed phase flow rates, are plotted in Figures 5 and 6 with compartment height as parameter. Similar graphs may be constructed using the other column variables as parameters. As shown in Figure 5, at dispersed phase flow rate of 20.44 ft./hr. holdup varied linearly with continuous phase flow rate; at dispersed phase flow rate of 40.87 ft./hr. holdup varied more rapidly with increasing flow rate of the continuous phase, as illustrated in Figure 6. This is apparently because all the former operations were in the region below loading, while the latter operations were in the region above loading. In general for a given column geometry and rotor speed the velocity of the dispersed phase had a more pronounced effect on the holdup of the solvent droplets than the continuous-phase velocity.

Reproducibility of Results

The holdup results at 0 rev./min for a specific column geometry are reproducible within 5 to 6% on a relative basis. The holdup data at other than 0 rev./min. with zero continuous-phase flow are also reproducible within 5 to 6%. However the results for constant dispersed-phase velocity and varying continuous-phase velocities at other than 0 rev./min. are generally reproducible within 9 to 10% on a relative basis. The internal consistency of the data is well illustrated in Figures 3 to 6.

CORRELATION OF RESULTS

As previously stated, based on the result of their study of a 3-in. rotating disk unit, Logsdail, Thornton, and Pratt (*6*) recommended the use of Equations (1) through (6) for the correlation and/or estimation of the behavior of rotating disk columns. Accordingly, values of two types of characteristic velocity were evaluated from the present data. The first type is referred to as $\overline{V_N}'$ and represents the characteristic velocity calculated for each run condition. The second type is denoted by $\overline{V_N}$, the term as used by Logsdail, Thornton, and Pratt to represent an average characteristic velocity at a given column geometry and rotor speed and for a variety of flow conditions.

Figure 7 shows the set of data at 461.8 rev./min. plotted in accordance with Equation (1) of Logsdail, Thornton, and Pratt. It is evident from the figure that for this particular set of data there is an effect of the continuous phase flow rate which has not been taken into account by the equation. However this effect of the continuous phase flow rate is not apparent for all column geometries, and in some cases Equation (1) satisfactorily correlates the data. In general the column geometries and rotor speeds studied in this investigation can be classified into four categories according to how well Equation (1) represents the holdup data at each of these combinations of column geometry and rotor speed:

1. Data obtained only at $V_c = 0$. $\overline{V_N}'$ remains relatively constant with varying V_d.
2. Data obtained only at $V_c = 0$. $\overline{V_N}'$ increases with increasing V_d.
3. $\overline{V_N}'$ increases with increasing V_d and V_c.
4. $\overline{V_N}'$ decreases with increasing V_c but remains relatively constant with varying V_d.

The runs at 0 rev./min. and unit A belong to the second group. The runs at 0 rev./min. and units B and H belong to the third class. The fourth category includes the runs at around 460 rev./min. for all units except unit G and the two sets of runs at around 200 rev./min. for units B and H. All other runs belong to the first group.

There is another criterion by which the column geometries and rotor speeds studied in this investigation can be divided into different categories, the behavior of the values of $\overline{V_N}$ with changes in column geometries and rotor speeds. It appears that the values of $\overline{V_N}$ remain constant below rotor peripheral speeds of about 300 ft./min. but decrease with increasing rotor peripheral speed above 300 ft./min. This is illustrated in Figure 8 in which

$\overline{V_N}$ is plotted vs. rotor peripheral speed for a given column geometry. The figure 300 ft./min. is by no means suggested as an absolute criterion to divide the zone of constant V_N from that in which $\overline{V_N}$ varies with rotor peripheral speed, particularly since only a single system has been used in this investigation. Rather it is pointed out as an observation to be investigated more fully by future workers.

Neither of the above phenomena was observed by Logsdail, Thornton, and Pratt (*6*), possibly owing to the difference in the ranges of the variables studied in this investigation and in those of Logsdail, Thornton, and Pratt. The holdup data for this investigation were determined at rotor speeds ranging from 0 to 632.9 rev./min., with rotor peripheral speeds ranging from 0 to 497.0 ft./min. The data of Logsdail, Thornton, and Pratt were determined at rotor speeds ranging from 500 to 1,600 rev./min., with rotor peripheral speeds ranging from 195 to 629 ft./min. However holdups were measured by Logsdail, Thornton, and Pratt only at rotor speeds between 900 and 1,200 rev./min., equivalent to rotor peripheral speeds between 354 and 471 ft./min. In measuring the dispersed-phase holdup the maximum superficial phase flow rates studied in this investigation were generally about twice as high as the maximum superficial phase flow rates studied by Logsdail, Thornton, and Pratt.

To improve the representation of the data by Equation (1) it appears that a promising procedure is to rewrite the equation as

$$\frac{V_d}{X} + \frac{k_1 V_c}{(1-X)} = \overline{V}\,(1-X) \quad (6)$$

Equation (6) can be derived by a procedure similar to that used by Logsdail, Thornton, and Pratt in developing Equation (1); however an effect of the continuous-phase velocity upon holdup must now be assumed. At $k_1 = 1.0$, Equation (6) reduces to Equation (1).

Figure 7 also shows the previous data plotted in accordance with Equation (6), with $k_1 = 2.1$. The improvement in correlation is obvious. Unfortunately the number of variations in each of the variables studied in this investigation was too small and the statistical experimental error too large to permit determination of whether a trend in k_1 existed with geometric configuration. However the holdup data obtained in this investigation at all units except A and H could be correlated to ± 20% with $k_1 = 1$ as per Logsdail, Thornton, and Pratt, while the data for units A and H could be

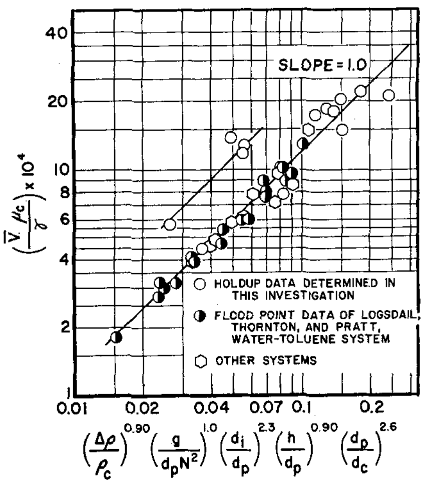

Fig. 9. Correlation of column holdup with physical properties and column geometry.

correlated to ± 20% with $k_1 = 2.1$. It is interesting to note that units A and H have in common a difference between disk and stator diameters of ¼ in., while all other units, except unit G, have difference between stator and disk diameters of 1 in. or more. For unit G, because of the small stator opening, the dispersed phase flows through the column in rivulets so that the column no longer behaves as an rotating disk unit.

In analyzing the data obtained in this investigation, and that obtained by earlier workers (*2, 6*) to determine the limits of applicability of Equations (5) and (6) in predicting or analyzing the performance of rotating disk columns, it was found that a better representation of the available data is obtained by

$$\frac{\overline{V}\mu_c}{\gamma} = K_1\left[\frac{\Delta\rho}{\rho_c}\right]^{0.90}\left[\frac{g}{dpN^2}\right]^{1.0}\left[\frac{di}{dp}\right]^{2.3}\left[\frac{h}{dp}\right]^{0.9}\left[\frac{dp}{dc}\right]^{2.6} \quad (7)$$

Equation (7) is essentially the same as Equation (5) except that the exponent on dp/dc is 2.6 instead of 2.7. This change is supported by the data of Reman and Olney (*2*), which gave an exponent on dp/dc of 2.60 when the data were reinterpreted by Logsdail, Thornton, and Pratt (*6*) in accordance with Equation (5). Also it should be recalled that Logsdail, Thornton, and Pratt used only data on a 3-in. column in arriving at the exponent 2.7. The data of this investigation, and that of Logsdail, Thornton, and Pratt are shown in Figure 9. The uppermost series of points represents those units having small stator and disk diameter differences and which required a $k_1 = 2.1$ in Equation (6).

It therefore appears that for purposes of correlation the dispersed-phase holdup data and the characteristic velocities evaluated from these data may be used as a criteria for estimating rotating disk column performance characteristics providing certain geometric and operational considerations are followed: that rotor peripheral speeds below 300 ft./min. seem requisite for constant characteristic velocities, and depending on whether $(di - dp)/dc$ is larger or smaller than 1/24, a k_1 value of 1.0 or 2.1, respectively, should be used in Equation (6) to give a good correlation of performance characteristics. It should be noted that all of the data of Logsdail, Thornton, and Pratt are obtained at column geometries with $(di - dp)/dc$ larger than 1/24.

SUMMARY OF RESULTS

1. At rotor peripheral speeds less than 300 ft./min. entrapment of dispersed-phase droplets under stator rings and/or rotor disks occurred. However generally the droplets are not trapped permanently and have a net movement through the column.

2. Based on the results of this study and the works of previous investigators (*2, 6*) the optimum operating conditions for rotating disk column units appear to exist over the following ranges of variables: (di/dc), 2/3 to 3/4; (dp/dc), 1/2 to 2/3; (h/dc), 1/3 to 1/2; rotor peripheral speed larger than 300 ft./min.; and flow rates either at loading point or at 50% of the flooding rates (neglecting solute effect).

3. The holdup data at a given column geometry and rotor speed have been related to the flow rates by

$$\frac{V_d}{X} + \frac{k_1 V_c}{1-X} = \overline{V}\,(1-X)$$

where $k_1 = 2.1$ at $(di - dp)/dx \leq 1/24$ and 1.0 at $(di-dp)/dc > 1/24$. The term $\overline{V}$ is a constant, is treated as a parameter, and is found to remain constant with varying rotor speeds at rotor peripheral speeds less than 300 ft./min.

4. The values of $\overline{V}$ estimated by the above equation from the present holdup data obtained at either 460 or 600 rev./min. have been correlated, along with the values of $\overline{V}$ estimated from the flood point data of Logsdail, Thornton, and Pratt (*6*), in terms of the column geometry, rotor speed, and physical properties of the system by

$$\left(\frac{\overline{V}\mu_c}{\gamma}\right) = K_1\left(\frac{\Delta\rho}{\rho_c}\right)^{0.90}\left(\frac{g}{dpN^2}\right)^{1.0}\left(\frac{di}{dp}\right)^{2.3}\left(\frac{h}{dp}\right)^{0.90}\left(\frac{dp}{dc}\right)^{2.6}$$

where $K_1 = 0.0225$ at $(di - dp)/dc \leq 1/24$, and 0.012 for $(di - dp)/dc > 1/24$. It therefore appears that flooding rates in a rotating disk column may be estimated from holdup data, and vice versa.

NOTATION

a = interfacial area of contact between two fluid phases
dc = inside diameter of the column
di = diameter of stator opening
dp = diameter of rotor disk
g = acceleration due to gravity
$(H.T.U.)_o$ = over-all height of a transfer unit
h = compartment height
K = over-all mass transfer coefficient
K_1 = coefficient in characteristic velocity correlation
k_1 = coefficient in holdup correlation
m = constant
N = speed of disk rotation
V = superficial liquid velocty, cu. ft./(hr.) (sq.ft. of column cross section)
$\overline{V}, \overline{V}_N$ = characteristic velocity (average) for a given system in a given column geometry and rotor speed, estimated from Equations (1) and (7) respectively, ft./hr.
$\overline{V}_N'$ = characteristic velocity estimated from Equation (1) for an individual run with a given system in a given column geometry and rotor speed, ft./hr.
X = fractional holdup of the dispersed phase in that portion of the column volume which may be occupied by liquid
μ = viscosity
γ = interfacial tension
ρ = density
$\Delta\rho$ = density difference between the dispersed and the continuous phase

Subscripts

c = continuous phase
d = discontinuous phase

LITERATURE CITED

1. Reman, G. H., *U.S. Patent 2,601,674.*
2. ———, and R. B. Olvey, *Chem. Eng. Progr.*, **51**, 141 (1955).
3. Reman, G. H., and J. G. van de Vusse, *Petrol. Refiner*, **34**, No. 9, p. 129 (1955).
4. ———, *Genie Chem.*, **74**, 106 (1955).
5. Vermijs, H. J. A., and H. Kramers, *Chem. Eng. Sci.*, **3**, 55 (1954).
6. Logsdail, D. H., J. B. Thornton, and H. R. C. Pratt, *Trans. Inst. Chem. Engrs. (London)*, **36**, 301 (1957).
7. Markas, S. E., D.Sc. thesis, Carnegie Inst. Technol., Pittsburgh, Pennsylvania (1955).

Manuscript received April 7, 1959; revision received November 21, 1960; paper accepted November 23, 1960. Paper presented at A.I.Ch.E. Atlantic City meeting.

Flow of Non-Newtonian Fluids in a Magnetic Field

TURGUT SARPKAYA

University of Nebraska, Lincoln, Nebraska

The analytical solution to the equation of motion is given for the steady laminar flow of a uniformly conducting incompressible non-Newtonian fluid between two parallel planes. The fluid is under the influence of a constant pressure gradient and is subjected to a steady magnetic field perpendicular to the direction of motion. Two non-Newtonian models are considered: the Bingham plastic model and the power-law model. Flow rates and the velocity profiles for various values of the Hartmann number and the generalized Hartmann number are presented and compared with those corresponding to Newtonian fluids.

Since the time of convenient creation of an ideal fluid to the present development of the applied science known as *rheology*, the restrictions imposed on the number of variables affecting the distribution of shear stress in a given flow have been relaxed systematically. In the past years several simple flow problems of classical hydrodynamics have received new attention in the more general context of magnetohydrodynamics. It is sufficient to mention in this connection the work of Hartmann and Lazarus (*1*) on the flow between two parallel walls, its extension to the case of flow in a straight pipe by Shercliff (*2, 3*), and the work of Bleviss (*4*) on the Couette flow. Evidently the inevitable extension of the study of the Newtonian fluid flow in the presence of a magnetic field to the flow of non-Newtonian fluids further relaxes the restrictions imposed on the shear stress and on the other characteristics of flow. It should be noted however that exact solutions for problems of this nature exist for special cases only. These cases may not correspond to a specific case of practical interest. The principal thought behind these investigations is that the significant physical features of the flow will stand out clearly, unobscured by a mathematical thicket, and that the results so obtained will serve as a good approximation to the physical model of interest in predicting the qualitative fluid behavior, and will guide one in facing more complicated situations.

The study of the motion of non-Newtonian fluids in the absence as well as in the presence of a magnetic field has applications in many areas. A few examples are the flow of nuclear fuel slurries, flow of liquid metals and alloys such as the flow of gallium at ordinary temperatures (30°C.), flow of plasma, flow of mercury amalgams,